Direct and Ozone-Mediated Forcing of the Southern Annular Mode by Greenhouse Gases

Olaf Morgenstern[1], Guang Zeng[1], Sam M. Dean[1], Manoj Joshi[2], N. Luke Abraham[3], and Annette Osprey[4]

Corresponding author: Olaf Morgenstern, National Institute of Water and Atmospheric Research, Lauder, New Zealand. (olaf.morgenstern@niwa.co.nz)

[1]National Institute of Water and Atmospheric Research, New Zealand

[2]School of Environmental Science, University of East Anglia, Norwich, UK

[3]NCAS-Climate, Department of Chemistry, University of Cambridge, UK

[4]NCAS-CMS, Department of Meteorology, University of Reading, UK

We assess the roles of long-lived greenhouse gases and ozone depletion in driving meridional surface pressure gradients in the southern extratropics; these gradients are a defining feature of the Southern Annular Mode. Stratospheric ozone depletion is thought to have caused a strengthening of this mode during summer, with increasing long-lived greenhouse gases playing a secondary role. Using a coupled atmosphere-ocean chemistry-climate model, we show that there is cancellation between the direct, radiative effect of increasing greenhouse gases by the also substantial indirect – chemical and dynamical – feedbacks that greenhouse gases have via their impact on ozone. This sensitivity of the mode to greenhouse-gas induced ozone changes suggests that a consistent implementation of ozone changes due to long-lived greenhouse gases in climate models benefits the simulation of this important aspect of Southern-Hemisphere climate.

1. Introduction

Variations in the Southern Annular Mode (SAM), as defined by the hemispheric pressure gradient between polar and extrapolar regions, affect the strength and position of the mid-latitude wind maximum (the "Roaring Forties"), and temperature and precipitation fields throughout the southern extratropics. A considerable increase in the frequency of occurrence of the positive phase of the SAM and associated blocking events [*O'Kane et al.*, 2013] during summer (December to February), observed during recent decades, thus means increased wind speeds over the Southern Ocean [*Thompson et al.*, 2011; *Abram et al.*, 2014; *WMO*, 2014]. In a mechanism understood to involve deep coupling of the stratosphere and troposphere, stratospheric ozone changes have influenced Southern-Hemisphere climate, from the tropics to the pole, causing an expansion of the tropical Hadley Cell and southward shifts of climate regimes [*Kang et al.*, 2011]. For the remainder of this century, models project some cancellation of these impacts of ozone depletion, set to reduce under ozone recovery, with those of further increases in long-lived greenhouse gases (GHGs), chiefly CO_2, CH_4, and N_2O [*IPCC*, 2013; *Zheng et al.*, 2013]. However, these GHGs do not just affect climate by trapping heat and influencing the equator-to-pole temperature gradient; they also have diverse impacts on ozone and its recovery. Increases in any of them, particularly CO_2, cool the stratosphere. This slows down gas-phase ozone-depleting reactions and generally leads to an acceleration of stratospheric overturning (the "Brewer-Dobson Circulation"), enhancing poleward transport of ozone [*WMO*, 2011, 2014]. Within the polar vortices, the cooling increases the prevalence of polar stratospheric clouds [*Roscoe and Lee*, 2001], which under contemporary, high-

chlorine conditions causes more polar ozone depletion. In combination, the GHG-induced cooling and accelerated overturning cause ozone to increase in mid-latitudes and to decrease in the tropics and seasonally over the poles [*Denman et al.*, 2007]. In addition to these dynamical and temperature effects, CH_4 and N_2O also affect chemistry. Increases in CH_4 reduce the rate of chlorine-catalysed ozone loss by promoting the return of chlorine to its reservoir form, hydrogen chloride (HCl), and also directly cause increased ozone production in the stratosphere in a catalytic process involving nitrogen oxides. N_2O increases, by contrast, induce ozone depletion by enhancing nitrogen-catalyzed ozone loss reactions [*Revell et al.*, 2012]. Anthropogenic emissions of N_2O now cause more ozone depletion than those of any of the ozone-depleting substances (ODSs) regulated under the Montreal Protocol [*Ravishankara et al.*, 2009]. Despite these known chemical and dynamical effects of the leading GHGs onto ozone, only a minority of models participating in the 5th Climate Model Intercomparison Project (CMIP5) calculated ozone interactively [*Eyring et al.*, 2013a], partly because including interactive stratospheric ozone chemistry has not been clearly shown to benefit the quality of climate simulations for non-chemical model fields [*Son et al.*, 2010], and because explicit ozone chemistry is a computationally expensive addition to climate models.

Here we investigate the roles of ozone depletion and long-lived GHGs in driving the Southern Annular Mode, differentiating between the above-discussed direct and indirect, ozone-mediated effects of GHG changes. For this we use a climate model, alternatively using interactive or prescribed ozone. The model ("NIWA-UKCA") is an atmosphere-ocean model, based on an early version of the HadGEM3-AO climate model, optionally including

an explicit stratosphere-troposphere chemistry scheme [*Morgenstern et al.*, 2009, 2013]. Apart from the interactive chemistry, the model is similar to the version described by *Hewitt et al.* [2011] but at a lower resolution in both the atmosphere (3.75° × 2.5°, 60 levels to 84 km) and the ocean ($\sim 2° \times 1°$, 31 levels). Relative to the model used by *Nowack et al.* [2014], there are only some differences in chemistry.

2. Experiments

Table 1 summarizes the experiments used here. The simulations all cover 1960-2100. The experiments using interactive ozone (REF-C2: all forcings; SEN-C2-fODS: ODSs fixed to their 1960 abundances; and SEN-C2-fGHG: GHGs fixed to their 1960 abundances) comply with corresponding definitions of the Chemistry-Climate Model Initiative [CCMI; http://www.met.reading.ac.uk/ccmi; *Eyring et al.*, 2013]. These simulations all use the same surface emissions of tropospheric ozone and aerosol precursors, and do not consider volcanic eruptions and solar variability.

In the SEN-C2-fODS simulations, where ODSs are held constant, we expect trends in ozone due to only the chemical and dynamical influences of the changing long-lived GHGs as discussed above, which may drive trends in the SAM. In the SEN-C2-fGHG simulation, where the long-lived GHGs are held constant, we expect only ozone depletion to influence the SAM. fOZONE uses a prescribed, annually periodic ozone field generated by ensemble- and time-averaging monthly-mean ozone fields from the first ten years of the five REF-C2 simulations. As such it will not contain changes in ozone, and any trend in the SAM can be attributed to only the radiative effects of the GHGs. NoIndir uses a prescribed ozone field generated by smoothing in time the monthly-mean ozone field

produced by SEN-C2-fGHG, in order to reduce the interannual variability in the field while retaining the annual cycle and the decadal-scale influence of ozone depletion. Thus in this experiment, trends in the SAM can be caused by ozone depletion or the direct radiative forcing of greenhouse gases but the indirect chemical and dynamical effects of changing greenhouse gases on ozone are absent. This suite of five experiments allows us to isolate the contributions not only of just changing GHGs or just changing ODSs, but also the benefits of including interactive chemistry. Hence both the direct and indirect (ozone-mediated) effects of GHG changes are present in the REF-C2 and SEN-C2-fODS experiments, but the indirect effect is suppressed in NoIndir and fOZONE. Therefore, differencing the REF-C2 and NoIndir experiments isolates this indirect effect.

Figure 1 shows effective equivalent stratospheric chlorine (EESC; a measure of the combined effect of chlorine and bromine onto ozone) [*Daniel et al.*, 2007] in the ODS scenario considered here [*WMO*, 2011], and total CO_2-equivalent radiative forcing [RF; a measure of the combined effect of anthropogenic greenhouse gases onto climate, *Forster et al.*, 2007] in the Representative Concentration Pathway (RCP) 6.0 [*Meinshausen et al.*, 2011]. These forcing functions are used in this analysis to represent in a simplified way the anthropogenic forcings (ozone depletion and longlived GHGs) applied in the model simulations. A regression analysis, detailed below, using these functions as basis functions can isolate the relative contribution of each to any trend in the SAM.

3. Results

An inspection of total-column ozone simulated by NIWA-UKCA shows that basically, the model produces a good representation of total-column ozone, with an annual cycle

similar to observations (figure 2). A small positive bias is within the usual range characterizing chemistry-climate models [*Austin et al.*, 2010]. The model produces ozone decline and subsequent recovery, caused by anthropogenic ozone depletion, some ozone super-recovery (i.e., late-century ozone abundances exceeding their 1960s values) in the Northern Hemisphere, caused by the impacts of increasing GHGs, and more intense ozone depletion in the fixed-GHG simulation (SEN-C2-fGHG) than in the reference experiment (REF-C2), suggesting that the model captures the partial cancellation of ozone depletion with the impact of increasing GHGs discussed above.

Next we assess surface pressure in these simulations. The SAM is an approximately ring-shaped feature with (for a positive SAM index) negative pressure anomalies over the South Pole and positive ones in a belt around mid-latitudes [e.g., *Gillett and Thompson*, 2003]. Hence here we define the SAM index as the difference in seasonal-, area-, and ensemble-mean surface pressure between mid- (38.75°S - 61.25°S) and polar latitudes (63.75°S - 90°S), minus the 1979-2012 mean of this quantity. This simple definition avoids complications to do with climatological drifts which affect other definitions based on empirical orthogonal function analysis [*Morgenstern et al.*, 2010].

Figure 3 shows the resulting SAM indices for the summer season. Similar to observations, for the period of 1960-2000 the REF-C2 ensemble-mean SAM index increases by about 3 hPa during this period. Relative to the ERA-Interim meteorological re-analyses [*Dee et al.*, 2011], the magnitude of the trend is likely underestimated. For the period after 2000, the REF-C2 simulations indicate little trend during summer, consistent with other modelling experiments that show some cancellation of the impacts of ozone recovery and

increasing GHGs [e.g., *Gillett and Fyfe*, 2013]. If underestimation of the 1960-2000 trend in REF-C2 is not a coincidence – our ensemble exhibits some considerable variability of this trend – it is consistent with an imperfect simulation of the SAM in our model. This might be the consequence of a cloud-radiative forcing bias over the Southern Ocean which is common in climate models [*IPCC*, 2013, and references therein]. A further investigation of this aspect is however beyond the scope of this paper.

We now perform a multiple linear regression analysis on the SAM indices, using as basis functions the large-scale forcing functions shown in figure 1. Details of the analysis are in the appendix. The resulting least-squares regression fits are depicted as violet lines in figure 3. Firstly, we note that in the experiments subject to both global warming and ozone depletion, both influences are of comparable magnitude (e.g., 1.68 ± 0.5 and 1.12 ± 0.46 hPa for REF-C2; the regression coefficients are given in figure 3). In the three experiments subject to ozone depletion (REF-C2, SEN-C2-fGHG, and NoIndir), the regression coefficients representing ozone depletion (given in green) are consistent with each other (namely 1.12 ± 0.46, 0.95 ± 0.75, and 0.82 ± 0.5 hPa), suggesting a reproducible trend in the SAM due to ODSs. The fixed-ozone (fOZONE) experiment produces a significant strengthening of the SAM (i.e., at 2.1 ± 0.42 hPa a positive regression coefficient with RF), which is significantly stronger than 1.05 ± 0.75 hPa which is found for the fixed-ODS (SEN-C2-fODS) experiment. Together, these two experiments suggest that the indirect, ozone-mediated influence of increasing GHGs onto the summer SAM offsets around half of the direct, radiative-forcing effect of increasing GHGs. (Note that the direct effect on the SAM of GHGs is present in both experiments, but their ozone-mediated,

indirect effect is only present in SEN-C2-fODS, see table 1). Hence, as a best estimate based on this analysis, we postulate that there is a 50% cancellation of the direct effect of GHG changes by the impact of ozone changes in SEN-C2-fODS.

We test this hypothesis using the other simulations. To assess whether the influence of the long-lived GHGs on the SAM is demonstrably larger in NoIndir than in REF-C2, we perform the regression on the difference in the SAM index between these two experiments. At -0.34 ± 0.70 hPa, with the uncertainty interval reflecting the 95% confidence limits, the resulting regression coefficient is less than 0 at about 83% confidence. We obtain numerically almost the same result if we replace NoIndir with fOZONE in this analysis $(-0.36 \pm 0.66$ hPa). Both results suggest that about 20% of the direct effect of increasing GHGs onto the SAM (as inferred from the fOZONE experiment) is offset by their impact on ozone. While this appears to be a smaller effect than the above-derived half cancellation, both results are within each others' respective 95% confidence intervals. There is considerable variability within each of the different ensembles for the regression coefficients, which makes it impossible to attribute this discrepancy to anything other than random variations.

4. Discussion

The analysis suggests that all three influences on the SAM in REF-C2 appreciably contribute towards its long-term trend, and that there is a sizeable cancellation between the direct and indirect effects of increasing GHGs onto the SAM. A caveat pertaining to this analysis is that this is just a single-model study which should be expanded into a multi-model analysis. Some of the simulations used here form part of a multi-model

intercomparison (CCMI) which will in time facilitate such an analysis. The magnitude of the effect is scenario-dependent; we have only studied one scenario [*Meinshausen et al.*, 2011; *WMO*, 2011] here.

However, if the above results are found to be robust, they would have important implications for large climate-model intercomparisons such as CMIP5 which informed *IPCC* [2013]. There, the majority of simulations used prescribed ozone climatologies [*Eyring et al.*, 2013a]. Considering the different sensitivities of stratospheric ozone to changes in CO_2, CH_4, and N_2O [*WMO*, 2014], the resulting trends in the SAM could depend on not just the combined radiative forcing of these gases, which is essentially what a climate model forced with prescribed ozone responds to, but also the specific assumptions made about the future evolutions of CH_4 and N_2O, increases of which have opposing chemical effects on ozone. This means scenario-specific ozone climatologies are required which are consistent with the GHG evolutions assumed in these scenarios [*Nowack et al.*, 2014]. Such consistency may be model-dependent, making it difficult to establish consistency across a range of different models. The findings presented here may increase the motivation to enter successors to CMIP5 (such as CMIP6) with coupled chemistry-climate models which by construction generate internally consistent ozone fields.

Appendix A: Details Of Regression Analysis

We stipulate that in REF-C2, the ensemble-average SAM index is the sum of five contributions:

$$t = \alpha r_{EESC} + (\beta_d + \beta_i)r_{RF} + \gamma + \rho \tag{A1}$$

Here, t is the ensemble-mean SAM index for one of our five experiments, r_{EESC} the dimensionless EESC regression function, r_{RF} is the dimensionless RF regression function (figure 1), α, β_d+ β_i are regression coefficients, quantifying the influences of ozone depletion and the direct and indirect GHG impacts, respectively, γ is the generally nonzero average of t, and $\rho = \mathcal{O}\left(n^{-1/2}\right)$ is the remainder not explained by the other terms, which scales with $n^{-1/2}$ (n = ensemble size). We calculate the coefficients performing a linear least-squares regression. Uncertainties are given relative to the 95% confidence interval. β_d and β_i are individually quantified by differencing the regression coefficients of pairs of experiments that include and exclude, respectively, the impact of changing GHGs on ozone, such as SEN-C2-fODS and fOZONE. To reduce uncertainty in the regression coefficients, in experiments in which either GHGs do not change or anthropogenic ozone depletion does not occur, the corresponding regression coefficients are assumed 0. For example, $\alpha = 0$ for SEN-C2-fODS. Such zero coefficients are omitted in figure 3.

The error calculation, which forms part of the above analysis, relies on two assumptions about the SAM indices: Residuals ρ need to be normally distributed, and autocorrelation needs to be small. Autocorrelation is addressed by applying the Durbin-Watson test [*Montgomery et al.*, 2001] to ρ:

$$d = \frac{\sum_{t=2}^{T}(\rho_t - \rho_{t-1})^2}{\sum_{t=1}^{T} \rho_t^2}, \tag{A2}$$

where $T = 140$ is the number of complete summer seasons in the time series for an experiment and ρ is the residual in the regression fit (equation A1). $d = 2$ would indicate no autocorrelation, whereas $d \approx 1$ would usually indicate significant autocorrelation. For the eight time series shown in figure 3 we find $1.85 < d < 2.06$. Hence we conclude that

autocorrelation does not significantly affect the regression analysis. Normality is assessed using a graphical approach: Figure 4 shows the cumulative distribution functions (CDF) for the five different experiments of the residuals ρ, expressed in multiples of their standard deviations σ. Residuals in all five ensemble averages satisfy essentially the same CDF which differs only slightly from a perfect Gaussian integral. Hence we can assume that the residuals are normally distributed.

The paper compares simulations with interactive ozone with other simulations driven with prescribed ozone. This opens up the question of whether a model driven with interactive ozone behaves differently from an equivalent model in which ozone is prescribed. We have conducted an additional ensemble of 4 simulations which are forced by the same GHG and ODS scenario as REF-C2 but ozone is not calculated interactively. Instead, it is prescribed as the smoothed ensemble- and monthly-mean ozone field of the REF-C2 experiment. Note that this ozone climatology is zonally varying. We have applied the analysis to these simulations as well. The resulting regression coefficients do not differ significantly from REF-C2, suggesting that whether ozone is interactive or prescribed does not – within the limits of statistical analysis inherent here – affect the slowly varying components of the SAM discussed in this work.

References

Abram, N. J., R. Mulvaney, F. Vimeux, S. J. Phipps, J. Turner, and M. H. England (2014), Evolution of the Southern Annular Mode during the past millennium, *Nature Climate Change*, 4, 564-569, doi:10.1038/nclimate2235.

Austin, J., et al. (2010), Decline and recovery of total column ozone using a multimodel time series analysis, *J. Geophys. Res.*, 115, D00M10, doi:10.1029/2010JD013857.

Bodeker, G. E., H. Shiona, and H. Eskes (2005), Indicators of Antarctic ozone depletion, *Atmos. Chem. Phys.*, 5, 2603-2615, www.atmos-chem-phys.org/acp/5/2603.

Daniel, J. S., G. J. M. Velders, et al. (2007), Halocarbon scenarios, ozone depletion potentials, and global warming potentials, Chapter 8 in *WMO: Scientific assessment of Ozone Depletion: 2006*, Global Ozone Research and Monitoring Project Report No. 50, Geneva, 39 pp.

Dee, D. P., et al. (2011), The ERA-Interim reanalysis: Configuration and performance of the data assimilation system. *Q. J. R. Meteorol. Soc.*, 137, 553 597, doi: 10.1002/qj.828

Denman, K. L., G. Brasseur, et al. (2007), Couplings between changes in the climate system and biogeochemistry. In: Climate Change 2007: The Physical Science Basis. Contribution of Working Group I to the Fourth Assessment Report of the Intergov-

ernmental Panel on Climate Change [Solomon, S., D. Qin, M. Manning, Z. Chen, M. Marquis, K.B. Averyt, M.Tignor and H.L. Miller (eds.)]. Cambridge University Press, Cambridge, United Kingdom and New York, NY, USA.

Eyring, V., et al. (2013) Overview of IGAC/SPARC Chemistry-Climate Model Initiative (CCMI) Community simulations in support of upcoming ozone and climate assessments, *SPARC Newsletter*, 40, 48-66.

Eyring, V., et al. (2013), Long-term ozone changes and associated climate impacts in CMIP5 simulations, *J. Geophys. Res. Atmos.*, 118, 5029-5060, doi:10.1002/jgrd.50316.

Forster, P., V. Ramaswamy, et al. (2007), Changes in atmospheric constituents and in radiative forcing, Chapter 2 of *Climate Change 2007: The Physical Science Basis. Contribution of Working Group I to the Fourth Assessment Report of the IPCC [Solomon, S., D. Qin, M. Manning, Z. Chen, M. Marquis, K. B. Averyt, M. Tignor and H. L. Miller (eds.)]*. Cambridge University Press, Cambridge, U.K. and New York, NY, USA.

Gillett, N. P., and D. W. J. Thompson (2003), Simulation of recent Southern Hemisphere climate change, *Science*, 302, 5643, 273-275, doi:10.1126/science.1087440.

Gillett, N. P., and J. C. Fyfe (2013), Annular mode changes in the CMIP5 simulations, *Geophys. Res. Lett.*, 40, 1189-1193, doi:10.1002/grl.50249.

Hewitt, H. T., D. Copsey, I. D. Culverwell, C. M. Harris, R. S. R. Hill, A. B. Keen, A. J. McLaren, and E. C. Hunke (2011), Design and implementation of the infrastructure of HadGEM3: the next-generation Met Office climate modelling system, *Geosci. Model Dev.*, 4, 223-253, www.geosci-model-dev.net/4/223/2011, doi:10.5194/gmd-4-223-2011.

Intergovernmental Panel on Climate Change (IPCC, 2013), Climate Change 2013, The Physical Science Basis, Working Group I Contribution to the Fifth Assessment Report of the Intergovernmental Panel on Climate Change, [Stocker, T. F., D. Qin, G.-K. Plattner, M. Tignor, S. K. Allen, J. Boschung, A. Nauels, Y. Xia, V. Bex, and P. M. Midgley (eds.)], Cambridge University Press, Cambridge, UK, and New York, NY, USA, 1535 pp.

Kang, S. M., L. M. Polvani, J. C. Fyfe, and M. Sigmond (2011), Impact of polar ozone depletion on subtropical precipitation, *Science*, 332, 6032, 951-954, doi:10.1126/science1202131.

Meinshausen, M., et al. (2011) The RCP greenhouse gas concentrations and their extensions from 1765 to 2300, *Climatic Change*, 109, 213-241, doi:10.1007/s10584-011-0156-z.

Montgomery, D. C., E. A. Peck, and G. G. Vining (2001), Introduction to Linear Regression Analysis, 3rd ed., New York, NY, J. Wiley & Sons.

Morgenstern, O., P. Braesicke, F. M. OConnor, A. C. Bushell, C. E. Johnson, S. M. Osprey, and J. A. Pyle (2009), Evaluation of the new UKCA climate-composition model – Part 1: The stratosphere, *Geosci. Model Dev.*, 2, 43-57, www.geosci-model-dev.net/2/43/2009.

Morgenstern, O., et al. (2010), Anthropogenic forcing of the Northern Annular Mode in CCMVal-2 models, *J. Geophys. Res.*, 115, D00M03, doi:10.1029/2009JD013347

Morgenstern, O., G. Zeng, N. L. Abraham, P. J. Telford, P. Braesicke, J. A. Pyle, S. C. Hardiman, F. M. OConnor, and C. E. Johnson (2013), Impacts of climate change, ozone recovery, and increasing methane on surface ozone and the tropospheric oxidizing

capacity, *J. Geophys. Res. Atmos.*, 118, 1028-1041, doi:10.1029/2012JD018382.

Nowack, P. J., N. L. Abraham, A. C. Maycock, P. Braesicke, J. M. Gregory, M. Joshi, A. Osprey, and J. A. Pyle (2014), A large ozone-circulation feedback and its implications for global warming assessments, *Nature Climate Change*, to appear, doi:10.1038/NCLIMATE2451.

O'Kane, T. J., J. S. Risbey, C. Franzke, I. Horenko, and D. P. Monselesan (2013), Changes in the meta-stability of the mid-latitude Southern Hemisphere circulation and the utility of non-stationary cluster analysis and split flow indices as diagnostic tools. *J. Atmos. Sci.*, 70, 824-842, doi:10.1175/JAS-D-12-028.1.

Ravishankara, A. R., J. S. Daniel, and R. W. Portmann (2009), Nitrous oxide (N_2O): The dominant ozone-depleting substance emitted in the 21st century, *Science*, 326, 123, doi:10.1126/science.1176985.

Revell, L. E., G. E. Bodeker, P. E. Huck, B. E. Williamson, and E. Rozanov (2012), The sensitivity of stratospheric ozone changes through the 21st century to N_2O and CH_4, *Atmos. Chem. Phys.*, 12, 11,309-11,317, doi:10.5194/acp-12-11309-2012.

Roscoe, H. K., and A. M. Lee (2001), Increased stratospheric greenhouse gases could delay recovery of the ozone hole and of ozone loss at southern mid-latitudes, *Adv. Space Res.*, 28, 7, 965970, doi:10.1016/S0273-1177(01)80025-9.

Son, S.-W., et al. (2010), Impact of stratospheric ozone on Southern Hemisphere circulation change: A multimodel assessment, *J. Geophys. Res.*, 115, D00M07, doi:10.1029/2010JD014271.

Thompson, D. W. J., and J. M. Wallace (2000), Annular modes in the extratropical circulation. Part I: Month-to-month variability, *J. Climate*, 13, 1000-1015.

Thompson, D. W. J., S. Solomon, P. J. Kushner, M. H. England, K. M. Grise, and D. J. Karoly (2011), Signatures of the Antarctic ozone hole in Southern Hemisphere surface climate change, *Nature Geosci.*, 4, 741-749, doi:10.1038/ngeo1296.

World Meteorological Organization (WMO, 2011), Scientific Assessment of Ozone Depletion: 2010, Global Ozone Research and Monitoring Project – Report No. 52, 516 pp., Geneva, Switzerland.

WMO (2014), Assessment for Decision-Makers: Scientific Assessment of Ozone Depletion: 2014, WMO, Global Ozone Research and Monitoring Project – Report No. 56, Geneva, Switzerland, http://www.wmo.int/pages/prog/arep/gaw/ozone_2014/ozone_asst_report.html.

Zheng, F., J. Li, R. T. Clark, and H. C. Nnamchi (2013), Simulation and projection of the southern hemisphere annular mode in CMIP5 models, *J. Climate*, 26, 9860-9879, doi:10.1175/JCLI-D-13-00204.1.

Table 1. NIWA-UKCA simulations used here.

Experiment	REF-C2	SEN-C2-fGHG	SEN-C2-fODS	fOZONE	NoIndir
Description	all forcings	fixed GHGs	fixed ODSs	fixed ozone	No GHG effect on ozone
No. of sims.	5	1	2	5	5
Ozone	Interactive	Interactive	Interactive	1960-1969 REF-C2 mean	SEN-C2-fGHG smoothed
Non-ODS GHGs	RCP 6.0	1960 abund.	RCP 6.0	RCP 6.0	RCP 6.0
ODSs	*WMO* [2011]	*WMO* [2011]	1960 abund.	1960 abund.	*WMO* [2011]
Effects present	OD, dGHG, iGHG	OD	dGHG, iGHG	dGHG	OD, dGHG

The first three experiments are as defined for the Chemistry-Climate Modelling Initiative (CCMI) [*Eyring et al.*, 2013]. OD = anthropogenic ozone depletion. dGHG = direct radiative effect of changing GHGs. iGHG = indirect, ozone-mediated effect of changing GHGs. Differencing REF-C2 and NoIndir, or SEN-C2-fODS and fOZONE, quantifies the iGHG effect. Note that all ozone climatologies used here are zonally variable.
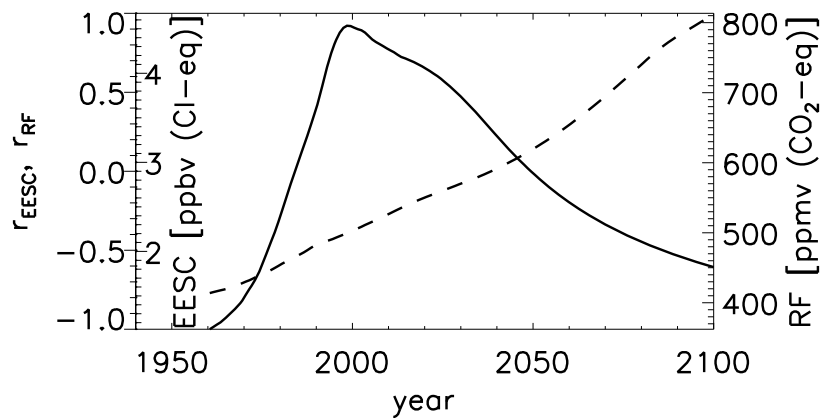
Figure 1. Regression functions used in the attribution analysis. Solid: EESC [*Daniel et al.*, 2007], indicating an increase from 1.1 to 4.5 parts per billion by volume (ppbv) of chlorine, followed by a decrease during the 21st century to 1.8 ppbv. Dashed: Combined CO_2-equivalent RF due to all long-lived GHGs in part per million by volume (ppmv) of CO_2, indicating a doubling during the course of the simulations. The non-dimensional scale (left) is used in the regression analysis for both regression functions. On this scale, both regression functions satisfy $\bar{r} = 0$ and $\max |r| = 1$.
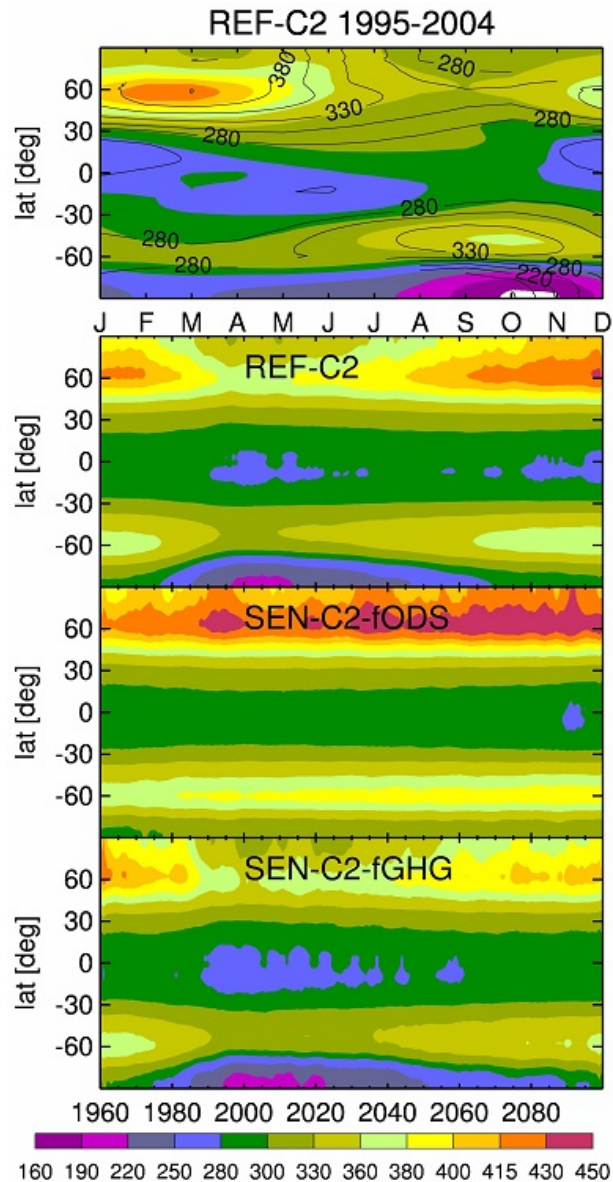
Figure 2. Zonal-mean total column ozone in the NIWA-UKCA simulations, in Dobson Units (DU). (top) Mean annual cycle for 1995-2004, from the REF-C2 ensemble average. Contours: NIWA assimilated satellite data [*Bodeker et al.*, 2005]. (2nd panel) REF-C2 Annual mean. (3rd panel) SEN-C2-fODS annual mean. (bottom) SEN-C2-fGHG annual mean.
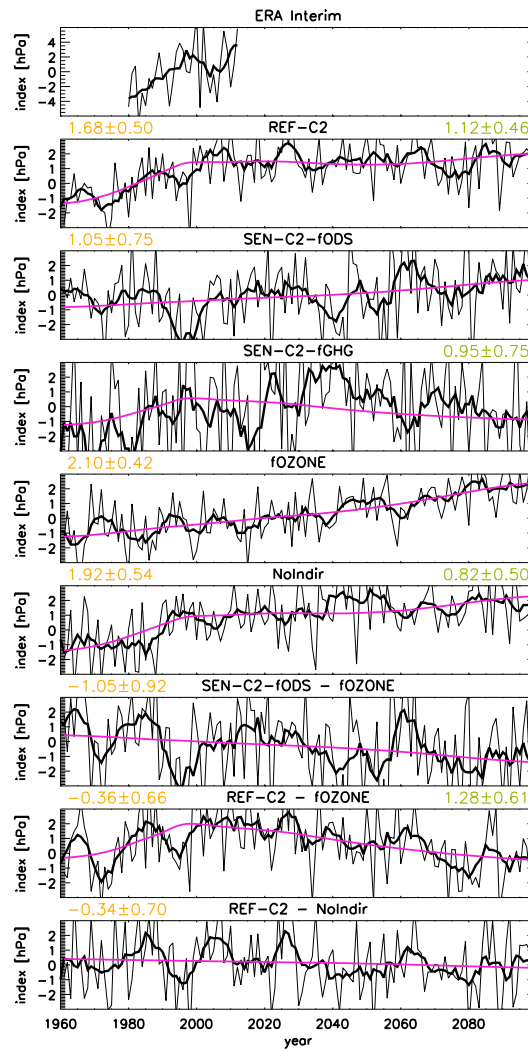
Figure 3. Seasonal SAM indices (hPa) for December-February. (thin black) Ensemble-average. (thick black) Ensemble-average, smoothed with 7-year boxcar filter. (violet) Least-squares regression fits using the EESC and RF explanatory functions. (orange) Regression coefficients against the non-dimensional radiative-forcing regression function (hPa; figure 1). (green) Same, but for the EESC regression function. Uncertainties refer to the 95% confidence level. Note the different scale applied to the ERA Interim panel.
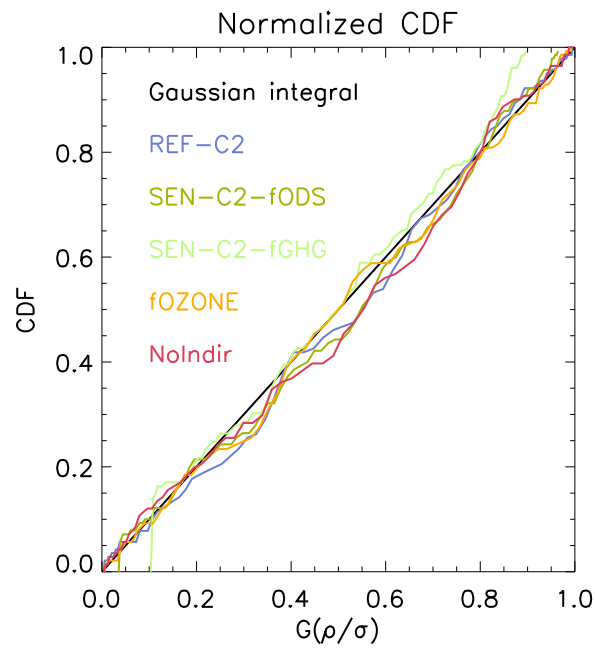
Figure 4. Cumulative distribution functions for the residuals ρ, displayed as $G(\rho/\sigma)$, where σ is the standard deviation of ρ and $G(x) = \frac{1}{\sqrt{\pi}} \int_{-\infty}^{x} \exp\left(-t^2\right) \mathrm{d}t$ is the Gaussian integral. Black: Perfect normal distribution. Colors: The five experiments.